https://doi.org/10.33263/Materials22.103110

ISSN: 2668-5728 https://materials.international

Materials International

Volume 2, Issue 2, Pages 0103-0110
2020

Received: 07.03.2020
Accepted: 07.04.2020
Published: 13.04.2020

Article

A Programmable Proton Exchange Membrane Fuel Cell Emulator Based on a DC-DC Synchronous Buck Converter

Chao-Tsung Ma [1,*], Zen-Yu Tsai [1], Chin-Lung Hsieh [2]

[1] Department of Electrical Engineering, CEECS, National United University, Miaoli 36063, Taiwan
[2] Institute of Nuclear Energy Research (INER), Atomic Energy Council, 1000 Wenhua Rd. Jiaan Village, Longtan District, Taoyuan City 32546, Taiwan

* Correspondence: ctma@nuu.edu.tw; Scopus ID: 55734816100

Abstract: In the development of fuel cell (FC) systems and related control technologies, it is convenient to employ FC emulators instead of using real FC systems for the testing of various FC characteristic parameters and operating conditions. This paper proposes a low-cost, fast-response, and programmable proton exchange membrane FC (PEMFC) hardware emulator based on a two-switch DC-DC synchronous buck converter and a digital signal processor (DSP) acting as a kernel controller. The V-I characteristics and control signals of the emulated PEMFC are determined through system analysis, modeling, and digitalization of the PEMFC model. The developed PEMFC model is then used to construct a programmable user-interface module through C programming. The programmable digital module can be directly embedded into the DSP for simulation studies and experimental tests on various hardware integrated implementations of FCs. Results obtained from simulations and hardware tests are in good consistent with each other and both prove the correctness and effectiveness of the developed converter based PEMFC emulator.

Keywords: proton exchange membrane fuel cell (PEMFC) emulator; digital signal processor (DSP); DC-DC synchronous buck converter.

1. Introduction

In recent years, people are paying more and more attention to the issue of greenhouse gas emissions. Therefore, there is little room left for further development of fossil fuel-based power generation. However, the energy demand for various industrial sectors continues to grow. Among the reported low-carbon power generation technologies, fuel cell (FC) is one of the fairly attractive options. A FC is a device that converts the chemical energy of hydrogen directly into electrical energy, and the resulting emissions are only heat and clean water. The main advantages of FCs include portability, high reliability, low pollutant emissions, and low maintenance requirements; it is recognized as a clean energy resource with high application flexibility. At present, there are a lot of research and

Cite This Article: Ma, C.T.; Tsai, Z.Y.; Hsieh, C.L. A Programmable Proton Exchange Membrane Fuel Cell Emulator Based on a DC-DC Synchronous Buck Converter. Mat Int **2020**, 2, 0103-0110.
https://doi.org/10.33263/Materials22.103110

publications related to FCs [1-8]. Although FC is a clean energy resource, the system's output is usually an unregulated low DC voltage. It is a basic processing stage to adjust the output voltage with a suitable power converter interface before the connection to a grid or a load.

When designing a FC power converter, typical considerations include the FC's nonlinear dynamics and steady state characteristics, which are strongly depending on the control technology used and the design parameters of each FC. Programmable FC emulator provides several advantages through digital formulation of FC types, environmental parameters, operating ranges, etc. Some mathematical models and simulation verification of proton exchange membrane FCs (PEMFCs) have been proposed in [9-13]. A Matlab/Simulink model was proposed in [9], and the effect of double-layer capacitor on the performance was also explored. The polarization equation of a humidified low-temperature PEMFC was proposed for all possible current densities and experimentally validated using a novel methodology in [10]. C. Restrepo et al. [11] proposed an improved diffusive model based on a finite-dimensional linear parameter-varying model and data of current inputs and voltage outputs. A 1.2-kW, Ballard Nexa FC was used to validate the advantages of the proposed model. D. Zhou et al. proposed two two-dimensional real-time models using tridiagonal matrix algorithm (Thomas algorithm) [12], validated using Ballard Nexa 1.2-kW FC, and a proposed secant algorithm [13] was validated using a computational COMSOL FC model. Hardware implementation of FC emulators can be found in [14-19]. In [14], a new software-hardware-integrated emulator was proposed based on electromotive force and internal impedance obtained through (1) constant current load characteristics and (2) step response characteristics + frequency characteristics, respectively. This model was later modified in [15] for a wider application frequency range. To match the power supply and the power requirement of an FC emulator, F. Flores-Bahamonde et al. [16] used a DC-DC non-inverting buck-boost converter-based DC transformer with a DC power supply. Ballard NEXA 1.2 kW diffusive FC model was used to validate the proposed method. In [17], a real-time FC emulator for Horizon H-500 was built based on a scaled-down electrical equivalent circuit. The mathematical and electrical models were simulated in MATLAB/Simulink environment, and then the implementation validated the design. A DC-DC buck converter was used in [18] as the FC emulator in MATLAB/Simulink environment with PI controller for voltage mode control. Relative humidity was considered in this design. P. A. Lindahl et al. [19] proposed a universal FC emulator that allowed simultaneous investigation of single cell and the entire hardware by employing a voltage amplifier whose input signal is the voltage output of a single cell. A single planar solid oxide FC (SOFC) was used to demonstrate the design. All of the abovementioned schemes, designed for a specific FC, are lacking application flexibility.

To eliminate the above disadvantage, this paper proposes a power converter based low-cost, fast-response and programmable PEMFC emulator. The proposed emulator adopts a two-switch DC-DC synchronous buck power converter as the main circuit and a DSP as the control core for achieving programmability and digital control mechanism. Following this introduction section, the basic principle of FC, FC's simple equivalent model, and a detailed equivalent model are introduced in the next section. In section three, the derivation of PEMFC models is explained, and an actual PEMFC characteristic curve is modeled and verified to obtain its output voltage-current (V-I) equation to be embedded into the DSP's interface module. In the fourth section, the accuracy and effectiveness of the proposed emulator are proven through typical simulation and experimental results. Finally, this paper is concluded in the last section.

2. Materials and Methods

2.1. PEMFC System.

The schematic of a FC system is shown in Fig. 1. In response to the need in addressing the systematic design procedure of a programmable FC emulator, this paper explores two PEMFC models, i.e. simplified model and detailed model [20].

2.1.1. Simplified PEMFCM model.

The simplified model of a PEMFC is shown in Fig. 2, including a controlled voltage source and a fixed resistance in series. The internal voltage of FC (E), Tafel slope (A), and voltage output of FC (V_{fc}) can be expressed as in (1)-(3).

$$E = E_{oc} - NA\ln(i_{fc}/i_0)\times 1/\left[(sT_d/3)+1\right]; \quad (1)$$

$$A = R\times T/(z\times\alpha\times F); \quad (2)$$

$$V_{fc} = E - R_{ohm}\times i_{fc}, \quad (3)$$

where R_{ohm} represents internal resistance (Ω), V_{fc} represents FC voltage (V), R = 8.3145 J/(mol*K), T_d represents response time (for 95% of final value) (s), F = 96485 A*s/mol, and z represents number of moving electrons (which equals 2).

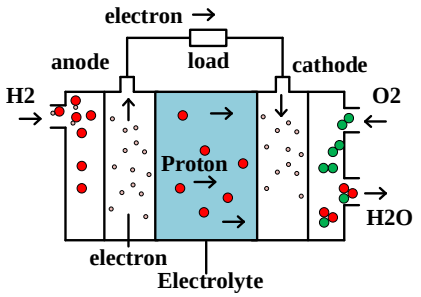

Figure 1. Schematic of a FC system.

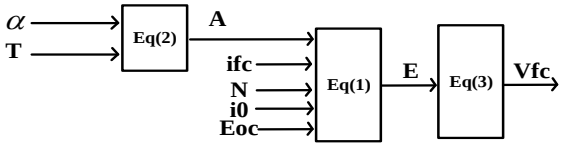

Figure 2. Simplified PEMFC model.

2.1.2 Detailed PEMFC Model.

The detailed model of PEMFC is shown in Fig. 3. To construct a detailed model, pressures, temperatures, compositions, and flow rates of air and fuel are all considered in the calculation. These parameter changes will directly affect Tafel slope, exchange current, and the open circuit voltage. The equivalent circuit of this model is roughly the same as the simplified model, with the difference being that pressures and flow rate as needed to update FC related parameters. The difference is that the user can input real-time pressures and flow rates to update related parameters. The detailed calculation for open-circuit voltage and exchange current is shown in (4) and (5), respectively.

$$E_{oc} = K_c \times E_n; \quad (4)$$

$$i_0 = \left\{\left[z\times F\times k\times(P_{H2}+P_{O2})\right]/Rh\right\}\exp(-\Delta G/RT), \quad (5)$$

where P_{O2} represents partial pressure of oxygen (atm), k = 1.38*10^{-23} (J/K), h = 6.626*10^{-34} (J*s), K_c is a constant under normal operation condition, E_n represents Nernst voltage (V), ΔG represents activation barrier (J), α represents charge transfer coefficient, T represents operating temperature (K), and P_{H2} represents partial pressure of hydrogen (atm). As shown in Fig. 3, blocks A, B, and C calculate the new values of E_{oc}, i_0, and A. First, block A determines the utilization rate of hydrogen and oxygen (U_{fH2} and U_{fO2}) as follows:

$$U_{fH2} = (6000\times R\times T\times i_{fc})/(z\times F\times P_{fuel}\times V_{fuel}\times x\times P_{std}) \quad (6)$$

$$U_{fO2} = (6000\times R\times T\times i_{fc})/(z\times F\times P_{air}\times V_{air}\times y\times P_{std}) \quad (7)$$

where P_{fuel} represents absolute supply pressure of fuel (atm), V_{air} represents air flow rate (l/min), P_{air} represents absolute supply pressure of air (atm), x represents composition percentage of hydrogen in the fuel (%), V_{fuel} represents fuel flow rate (l/min), and y represents composition percentage of oxygen in the oxidant (%).

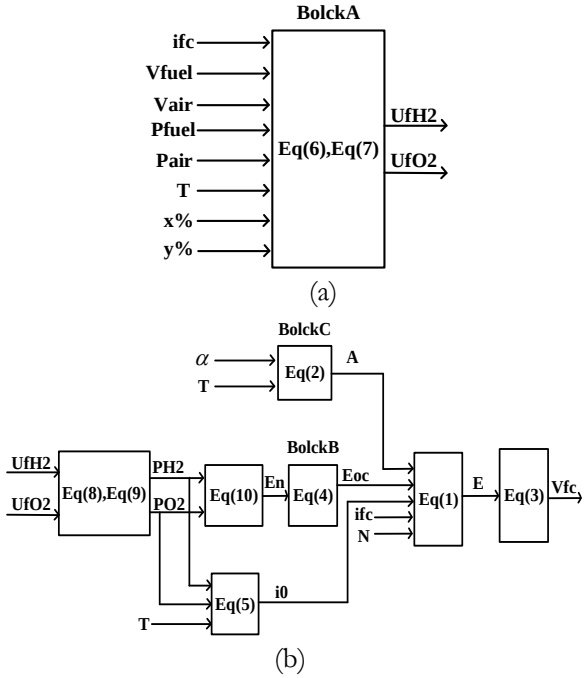

Figure 3. (a) & (b) are the detailed PEMFC model.

Partial pressures and Nernst voltage and be determined in block B as follows:

$$P_{H2} = \left(1 - U_{fH2}\right) \times x \times P_{fuel} \; ; \quad (8)$$

$$P_{O2} = \left(1 - U_{fO2}\right) \times y \times P_{air} \; ; \quad (9)$$

$$E_n = 1.229 + \left(T - 298\right) \times \left[\left(-44.43 + RT\right) / zF\right] \times \ln\left(P_{H2} \times \sqrt{P_{O2}}\right) \quad (10)$$

2.1.3 Circuit Architecture and control of FC Emulator.

Figure 4 shows the main circuit of the proposed FC emulator, where the calculation module is able to output a voltage signal based on Tafel slope, number of FCs, open-circuit voltage, exchange current, and FC current. The voltage signal is sent to the DSP to control the DC-DC converter. The emulated FC voltage output will then be obtained.

2.2. Design of DC-DC Synchronous Buck Converter.

The schematic of a DC-DC synchronous buck converter is shown in Fig. 5. The operating principle of the converter is described as follows: the high-frequency switching of the power transistors S1 and S2, combined with the output inductance and capacitance, outputs a voltage lower than the input voltage. By controlling the on time and off time (T_{on} and T_{off}) of the main switch, the DC output voltage of the converter can be controlled. The pulse width modulation (PWM) with a fixed switching period (T_s) and variable t_{on} are used for this purpose.

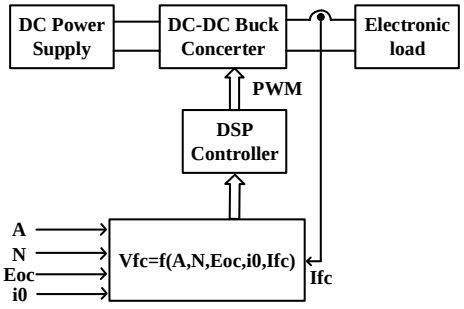

Figure 4. Block diagram of PEMFC emulator.

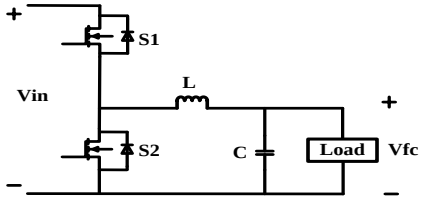

Figure 5. Schematic of the DC-DC synchronous buck converter.

The relationship between the input and output voltages is as follows:

$$V_{fc} = D \times V_{in}, \quad (11)$$

where the duty cycle (D) is as follows:

$$D = t_{on} / T_s. \quad (12)$$

When S1 is on, the voltage across the inductor L is

$$V_L(t) = L di_L / dt = V_{in} - V_{fc}. \quad (13)$$

During on period, inductor current increases from i_{L_min} to i_{L_max}, where

$$i_{L\min} = i_L(0) = V_{fc} / R_{fc} - \Delta I / 2, \quad (14)$$

and

$$i_{L\max} = i_L(DT) = V_{fc} / R_{fc} + \Delta I / 2, \quad (15)$$

where R_{fc} represents FC resistance. Capacitor current i_C is as follows:

$$i_C = i_L(T) - i_R(T) = I_L(t) - V_{fc} / R \; ; \quad (16)$$

$$i_C(0) = -\Delta I / 2 \; ; \quad (17)$$

$$i_C(DT) = \Delta I / 2. \quad (18)$$

Because of the linear change of i_C, the average inductor current is half of the peak value of the triangle wave. The peak value of the triangular wave is $\Delta I/2$ and thus equals $\Delta I/4$. According to average current in half of the period, the output voltage change ΔV can be expressed as follows:

$$\Delta V = \left(I_C \times T / 2\right) / C = \Delta I \times T / 8C = \Delta I / 8fC \quad (19)$$

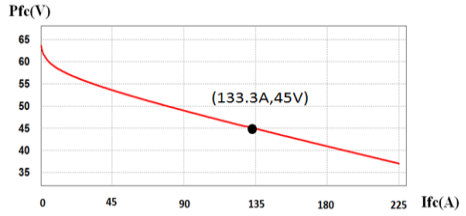

(a)

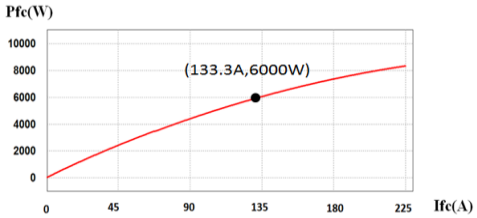

(b)

Figure 6. (a) & (b) are the verification results of the proposed FC model.

In order to improve output current ripple, a low pass filter (LPF) can be used to help suppress the variations. In addition, using a switch S2 in parallel with the filter solves the efficiency issue related to filter inductance discharge, giving it a low-resistance path to discharge while S1 is off. As shown in Fig. 5, while is S1 on, and S2 is off, the body diode of S2 is off because of the revers bias, and thus the energy is sent to the inductor, the capacitor, and the load; while S1 is off, and S2 is on, the current is able to freewheel, sending the energy stored in the inductor to the output terminal.

2.3. FC Model Verification.

The model parameters in [20] are first adopted to verify the correctness of the proposed FC mathematical model. For steady state fixed-point verification, the nominal operation parameters are as follows: FC voltages at 0 A and 1 A [E_{oc},V_1] = [65,63], nominal operation point [I_{nom},V_{nom}] = [133.3,45], maximum operation point [I_{max},V_{min}] = [225,37], nominal FC stack efficiency = 55%, number of FCs in series N = 65, operation temperature = 65 °C, nominal air flow rate $V_{air(nom)}$ = 297 l/min, nominal compositions of fuel and air [x_{nom},y_{nom}] = [99.999%,21.1%], and nominal supply pressures [P_{H2},P_{air}] = [1.5,1]. The verification results are shown in Fig. 6. The proposed model is capable of accurately calculating the FC V-I curve, proving the correctness of this module.

3. Results and Discussion

3.1. Simulation and Hardware Implementation Results.

This section verifies the characteristics of the proposed 110W PEMFC mathematical model and the hardware emulator at different temperatures through simulation and implementation measurements. The specifications of experimental circuit and measuring devices for the proposed PEMFC emulator are as follows: voltage input V_{in} = 200 V, buck inductance L = 500 µH, output capacitance C = 47 µF, maximum short circuit current $I_{sh,max}$ = 5.5 & 7.5 (A), and maximum open circuit voltage $V_{oc,max}$ = 42 & 45.67 (V).

Figure 7. Photo of the constructed PEMFC emulator.

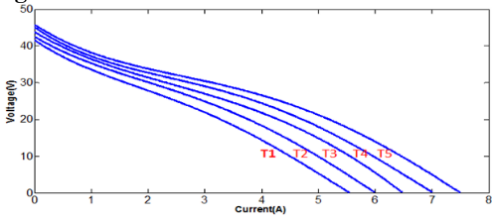

(a)

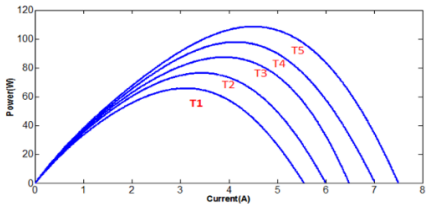

(b)

Figure 8. Simulation results of PEMFC emulator at 5 different operating temperatures, T_1~T_5 (45°C, 55°C, 65°C, 75°C, 85°C): (a) V-I curves, and (b) P-I curves.

Figure 7 shows the experimental setup and measuring devices, and Fig. 8 shows the simulation results of V-I and P-I curves using Matlab at the different operating temperatures.

The hardware implementation test is performed at two operating temperatures: 45°C and 85 °C. Figs. 9 & 10 show the comparison between simulated and implemented V-I and P-I curves of the proposed PEMFC emulator at 45°C operating temperature, respectively (I_{fc}: 2A/div; V_{in}: 2V/div; P_{fc}: 2W/div; T: 1s/div).

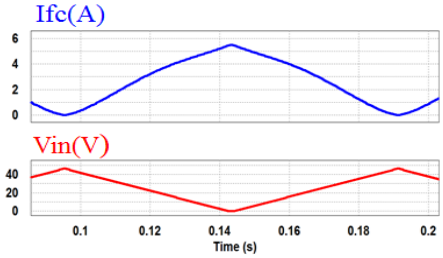

(a)

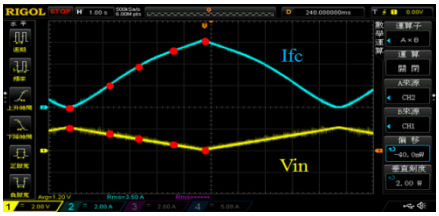

(b)

Figure 9. V-I characteristic of the proposed PEMFC emulator at 45°C: (a) simulation results, and (b) implementation results.

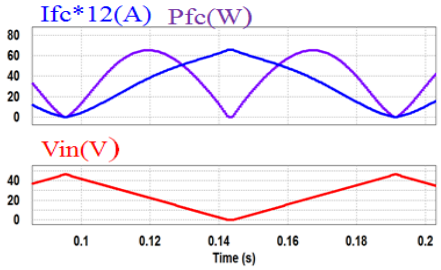

(a)

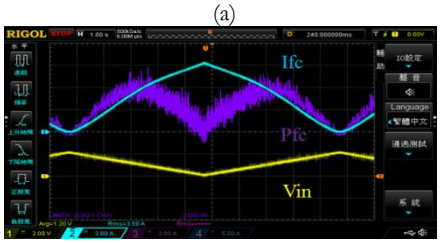

(b)

Figure 10. P-I characteristic of the proposed PEMFC emulator at 45°C: (a) simulation results, and (b) implementation results.

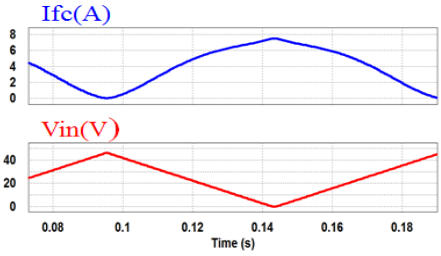

(a)

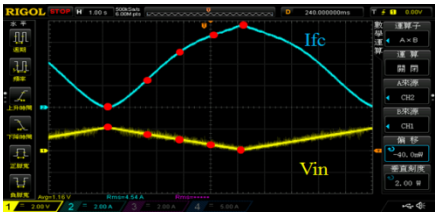

(b)

Figure 11. V-I characteristic of the proposed PEMFC emulator at 85°C: (a) simulation results, and (b) implementation results.

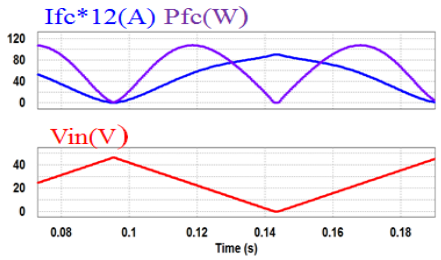

(a)

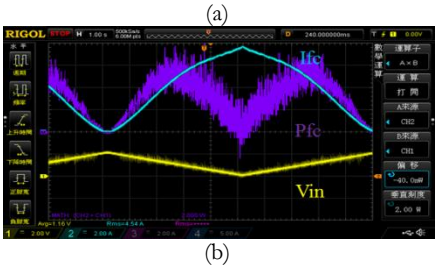

(b)

Figure 12. P-I characteristic of the proposed PEMFC emulator at 85°C: (a) simulation results, and (b) implementation results.

Figs. 11 & 12 show the comparison between simulated and implemented V-I and P-I curves of the proposed PEMFC emulator at 85°C operating temperature, respectively (I_{fc}: 2A/div; V_{in}: 2V/div; P_{fc}: 2W/div; T: 1s/div).

4. Conclusions

This paper has successfully developed an 110W, low-cost, programmable PEMFC emulator. The proposed PEMFC hardware emulator employs a DC-DC synchronous buck converter as the main circuit and a DSP as the digital controller to achieve fast tracking of the dynamic V-I characteristics of a real PEMFC and to achieve the feature of programmable emulation mechanisms. In the processes of emulation, the real-time voltage commands, the corresponding output voltage values of a given PEMFC operating conditions, were calculated using a derived mathematical model that considers the pressure, temperature, composition percentage, and flow rate of both fuel and air. A programmable digital user interface was then constructed through a C programming module. The correctness and effectiveness of the proposed PEMFC emulator have been tested through simulation at different operating temperatures and verified with hardware implementation at two operating temperatures.

Funding

This research is mainly funded by the Ministry of Science and Technology (MOST) of Taiwan via the following contract: MOST 108-2221-E-239-007.

Acknowledgments

The authors would like to thank the Ministry of Science and Technology (MOST) of Taiwan (MOST 108-2221-E-239-007) and the Institute of Nuclear Energy Research (INER), Atomic Energy Council, of Taiwan for supporting the energy related researches regarding key technologies and the design of advanced power and energy systems.

Conflicts of Interest

The authors declare no conflict of interest.

References

1. Alrewq, M.; Albarbar, A. Investigation into the characteristics of proton exchange membrane fuel cell-based power system. *IET Science, Measurement & Technology* **2016**, *10*, 200-206, https://doi.org/10.1049/iet-smt.2015.0046.
2. Ahmad, M.; Ahmad, B.; Harrison, R.; Ramis, B.; Meredith, J.; Bindel, A.; Martinez Lastra, J.L. A knowledge-based approach for the selection of assembly equipment based on fuel cell component characteristics; In Proceedings of the IECON 2015; https://doi.org/10.1109/IECON.2015.7392230.
3. Rahman, M.A.; Shawon, M.H.; Sohel, I.H. Comparative analysis of control schemes with harmonic characteristics for fuel cell system. 8th International Conference on Electrical and Computer Engineering, Dhaka, 2014, pp. 615-618, https://doi.org/10.1109/ICECE.2014.7026981.
4. Minarik, D.; Moldrik, P.; Meadowcroft, T. Experimental validation of solid oxide fuel cell's basic operational characteristic. In Proceedings of the 2014 15th International Scientific Conference on Electric Power Engineering (EPE), 12-14 May 2014; pp. 315-319, https://doi.org/10.1109/EPE.2014.6839525.
5. Choi, K.; Ahn, J.; Lee, J.; Vinh, N.D.; Kim, H.; Park, K.; Hwang, G. An Experimental Study of Scale-up, Oxidant, and Response Characteristics in PEM Fuel Cells. *IEEE Transactions on Energy Conversion* **2014**, *29*, 727-734, https://doi.org/10.1109/TEC.2014.2322877.
6. Zhou, M.; Prasad, J.V.R. Transient characteristics of a fuel cell powered UAV propulsion system. In Proceedings of 2013 International Conference on Unmanned Aircraft Systems (ICUAS), 28-31 May 2013; pp. 114-123, https://doi.org/10.1109/ICUAS.2013.6564680.
7. Murooka, S.; Tomoda, K.; Hoshi, N.; Haruna, J.; Cao, M.; Yoshizaki, A.; Hirata, K. Consideration on fundamental characteristic of hydrogen generator system fueled by NaBH4 for fuel cell hybrid electric vehicle. In Proceedings of 2012 IEEE International Electric Vehicle Conference, 4-8 March 2012; pp. 1-6, https://doi.org/10.1109/IEVC.2012.6183289.
8. Katayama, N.; Tanaka, K.; Kogoshi, S. Sensitivity analysis on frequency characteristics of a fuel cell-electrical double layer capacitor hybrid power source system. In Proceedings of 2012 IEEE International Electric Vehicle Conference, 4-8 March 2012; pp. 1-5, https://doi.org/10.1109/IEVC.2012.6183269.
9. Chavan, S.L.; Talange, D.B. Modeling and simulation of effect of double layer capacitance on PEM fuel cell performance. In Proceedings of 2017 7th International Conference on Power Systems (ICPS), 21-23 Dec. 2017; pp. 259-264, https://doi.org/10.1109/ICPES.2017.8387303.
10. Thosar, A.; Agarwal, H.; Govarthan, S.; Lele, A. Comprehensive analytical model for polarization curve of a PEM fuel cell and experimental validation. *Chemical Engineering Science* **2019**, *206*, https://doi.org/10.1016/j.ces.2019.05.022.
11. Restrepo, C.; Garcia, G.; Calvente, J.; Giral, R.; Martínez-Salamero, L. Static and Dynamic Current–Voltage Modeling of a Proton Exchange Membrane Fuel Cell Using an Input–Output Diffusive Approach. *IEEE Transactions on Industrial Electronics* **2016**, *63*, 1003-1015, https://doi.org/10.1109/TIE.2015.2480383.
12. Zhou, D.; Gao, F.; Breaz, E.; Ravey, A.; Miraoui, A. Tridiagonal Matrix Algorithm for Real-Time Simulation of a Two-Dimensional PEM Fuel Cell Model. *IEEE Transactions on Industrial Electronics* **2018**, *65*, 7106-7118, https://doi.org/10.1109/TIE.2017.2787598.
13. Zhou, D.; Gao, F.; Al-Durra, A.; Breaz, E.; Ravey, A.; Miraoui, A. Development of a Multiphysical 2-D Model of a PEM Fuel Cell for Real-Time Control. *IEEE Transactions on Industry Applications* **2018**, *54*, 4864-4874, https://doi.org/10.1109/TIA.2018.2839082.
14. Reddy, B.M.; Samuel, P. Technology Advancements and Trends in Development of Proton Exchange Membrane Fuel Cell Hybrid Electric Vehicles in India: A Review. *Journal of Green Energy* **2017**, 7, 361-384, https://doi.org/10.13052/jge1904-4720.732.

15. Fukuoka, K.; Yamamura, N. Parameter Identification and Verification of the Fuel Cell Emulator. In Proceedings of 2018 21st International Conference on Electrical Machines and Systems (ICEMS), 7-10 Oct. 2018; pp. 850-853, https://doi.org/10.23919/ICEMS.2018.8549440.
16. Flores-Bahamonde, F.; Rivera, M.; Baier, C.; Calvente, J.; Giral, R.; Restrepo, C. DC transformer based on the versatile DC-DC noninverting buck-boost converter for fuel cell emulation. In Proceedings of 2017 IEEE Southern Power Electronics Conference (SPEC), 4-7 Dec. 2017; pp. 1-6, https://doi.org/10.1109/SPEC.2017.8333636.
17. Azri, M.; Khanipah, N.H.A.; Mubin, A.N.A.; Zukeri, M.Z.C.; Ibrahim, Z.; Rahim, N.A. Development of PEMFC emulator using electrical equivalent circuit. In Proceedings of 2017 6th International Conference on Electrical Engineering and Informatics (ICEEI), 25-27 Nov. 2017; pp. 1-6, https://doi.org/10.1109/ICEEI.2017.8312363.
18. Voottipruex, K.; Sangswang, A.; Naetiladdanon, S.; Mujjalinvimut, E.; Wongyoa, N. PEM fuel cell emulator based on dynamic model with relative humidity calculation. In Proceedings of 2017 14th International Conference on Electrical Engineering/Electronics, Computer, Telecommunications and Information Technology (ECTI-CON), 27-30 June 2017; pp. 529-532, https://doi.org/10.1109/ECTICon.2017.8096291.
19. Lindahl, P.A.; Shaw, S.R.; Leeb, S.B. Fuel Cell Stack Emulation for Cell and Hardware-in-the-Loop Testing. *IEEE Transactions on Instrumentation and Measurement* **2018**, *67*, 2143-2152, https://doi.org/10.1109/TIM.2018.2814070.
20. Tremblay, S.N.M.O.; Dessaint, L. A generic fuel cell model for the simulation of fuel cell vehicles. In Proceedings of 2009 IEEE Vehicle Power and Propulsion Conference, 7-10 Sept. 2009; pp. 1722-1729, https://doi.org/10.1109/VPPC.2009.5289692.